

# Validation of an agent-based building evacuation model with a school drill

Alan Poulos<sup>a,b,\*</sup>, Felipe Tocornal<sup>a,b</sup>, Juan Carlos de la Llera<sup>a,b</sup>, Judith Mitrani-Reiser<sup>c</sup>

<sup>a</sup>*Department of Structural and Geotechnical Engineering, Pontificia Universidad Católica de Chile, Santiago, Chile*

<sup>b</sup>*National Research Center for Integrated Natural Disaster Management CONICYT/FONDAP/15110017, Santiago, Chile*

<sup>c</sup>*Department of Civil Engineering, Johns Hopkins University, Baltimore, Maryland, USA*

---

## Abstract

An effective evacuation of buildings is critical to minimize casualties due to natural or anthropogenic hazards. Building evacuation models help in preparing for future events and shed light on possible shortcomings of current evacuation designs. However, such models are seldom compared or validated with real evacuations, which is a critical step in assessing their predictive capacities. This research focuses on the evacuation of a K-12 (kindergarten to 12th grade) school located within the tsunami inundation zone of Iquique, Chile. An agent-based evacuation model was developed to simulate the evacuation of approximately 1500 children and staff from the school during a global evacuation drill carried out for the entire city. The model simulates the motions of heterogeneous human agents, and the simulations were validated using video analysis of the real event. Resulting error estimations between predicted versus measured flow rates and evacuation times are 13.5% and 5.9%, respectively. The good agreement between the simulated and measured values can be attributed to the known distribution of students and staff at the start of the drill, and their known exposure to emergency preparedness protocols. However, the results presented herein show that this mathematical evacuation model can be used for logistical changes in the emergency planning.

Keywords: evacuation model; evacuation drill; agent-based modeling; human behavior.

## 1. Introduction

Several natural and anthropogenic hazards require people evacuation to safety zones in order to protect lives. Past experience has shown that evacuations may be ineffective and cause a significant number of deaths. For instance, in the last 20 years tsunami inundations generated by large earthquakes have killed more than 250,000 people (Guha-Sapir et al., 2016), most of them attributed to the Indian Ocean tsunami in 2004. Moreover, engineered defences are not sufficient in the case of large natural hazards, as evidenced by the 2011 Tohoku earthquake (Fraser et al., 2013). Consequently, developing the capacity to study evacuations beforehand is crucial to minimize casualties during these events.

The study of evacuation processes can be approached analytically (i.e., by numerical models) or experimentally (i.e., by means of evacuation drill exercises). Apart from its positive training effect, drills provide valuable information to understand the evacuation process and foresee potential problems during real events. However, they also have some drawbacks, such as the need for human and material resources, the impossibility of being performed at the design phase of infrastructure and to reflect the real state of stress of the evacuees. Simulation based numerical evacuations models have several advantages, an important one, the

---

\*Corresponding author.

Email addresses: [ajpoulos@uc.cl](mailto:ajpoulos@uc.cl) (Alan Poulos), [ftocorn1@uc.cl](mailto:ftocorn1@uc.cl) (Felipe Tocornal), [jcllera@ing.puc.cl](mailto:jcllera@ing.puc.cl) (Juan Carlos de la Llera), [jmitrani@jhu.edu](mailto:jmitrani@jhu.edu) (Judith Mitrani-Reiser)

possibility to anticipate problems with the design of current infrastructure and evacuation strategies at different physical scales, from single buildings to complete cities. Consequently, evacuation models have been used in the literature to study the design and management of the transportation systems that support evacuation processes, such as to study the effect of changing the architectural design of buildings to improve pedestrian traffic outflow (Shiwakoti and Sarvi, 2013), the choice of different modes of transportation and availability of vertical evacuation shelters for tsunami evacuations (Wang et al., 2016), and encouraging the collaboration between evacuees as a way of decentralizing evacuation management (Richter et al., 2013). However, like for any mathematical model, evacuation models need empirical validations before they can be used in prediction.

Most validations of pedestrian dynamic models have been qualitative, such as reproducing the collective phenomena of lane formation and oscillations at bottlenecks (Helbing et al., 2002), and only very few quantitative validations have been carried out due to the scarcity and unreliability of the available empirical data (Schadschneider et al., 2011). Moreover, comparisons performed quantitatively are normally at a small scale, such as movement along corridors (Sano et al., 2011) and in corners (Schadschneider et al., 2011), as well as evacuations from a single room (Lu et al., 2017; Helbing et al., 2003; Zhang et al., 2008; Lovreglio et al., 2014). Bigger scale comparisons are scarce and typically study the total evacuation time, disregarding the evacuation history (e.g., Olsson and Regan, 2001).

Therefore, this research focuses on the emergency evacuation of a K-12 school in the city of Iquique, Chile, during a training tsunami evacuation drill performed in August 2013 (08-A drill). More than 1500 students and staff evacuated the facility during the drill and were monitored using video cameras for validation purposes. The school was selected as a testbed for its large number of occupants, and since the age and location of the people at the beginning of the drill are known. The event occurred prior to the  $M_w$  8.2 earthquake of April 1<sup>st</sup>, 2014 in Pisagua, 94 km northwest from Iquique. This earthquake liberated less than 20% of the energy stored in the seismic gap defined between latitude 18°S in southern Peru and latitude 23°S in northern Chile (Lay et al., 2014), which had not been active since the 1877 earthquake (Chlieh et al., 2004). In this region, the Nazca Plate goes under the South American continental plate at a rate of about 68 mm/year. Because of the geometry of the subducting plate dipping at 18°, large megathrust earthquakes in this region are normally followed by a tsunami. Based on the Pisagua earthquake, the expected arrival time of the first tsunami waves is within 15 minutes (Catalán et al., 2015).

Early pedestrian dynamic models took advantage of some similarities between the movement of pedestrian crowds and fluids, thus proposing models based on fluid-dynamics and gas-kinetics (Henderson, 1971; Helbing, 1992). This modeling approach has a macroscopic resolution, since the smallest unity that can be modeled is the flow itself, which cannot consider explicitly the interactions between heterogeneous individuals. These models have produced reasonable results for high crowd densities, but are of limited value for densities smaller than 4 persons per  $m^2$  (Hughes, 2002).

More recent evacuation models have used a microscopic resolution, where the smallest unit that can be modeled is an individual. These models can be subdivided into continuous and discrete space problems, depending on how they consider the domain in which the individuals move. One of the most important continuous approaches is the social force model, first introduced by Helbing and Molnar (1995), which models pedestrians subjected to forces as particles following Newton's second law of motion. The forces represent effects such as: the desire to move to a destination; the collision avoidance with other pedestrians; the preservation of a minimum distance from obstacles; and the attraction to other agents. The model has also been extended to include panic (Helbing et al., 2000), and to eliminate overlapping between pedestrians (Lakoba et al., 2005). On the other hand, the most widely used microscopic discrete technique to simulate human evacuation are cellular automata models (Pelechano and Malkawi, 2008). These models divide the space in a grid, normally a two-dimensional tessellation using a regular polygon. Each cell of the grid has a state, which could represent in an evacuation model the presence of an individual in the cell or not, and a set of variables that are updated at each time step according to a set of local rules.

Agent-based modeling is a microscopic simulation technique that conceives a system as a collection of autonomous decision-making entities denoted as agents. At each time instant, each agent individually assesses its surrounding environment and makes decisions on the basis of a set of rules (e.g., Bonabeau, 2002). The dynamic properties of the system are assessed by running computer simulations of the model, and can result in the emergence of complex behaviors that cannot be predicted by modeling techniques that describe systems in equilibrium (Arthur, 2006). Some advantages of using these models are the capacity to include heterogeneity, randomness, and interactions at the agent level with relative ease. ABM has been used to

study the evacuation of humans during several hazards, including flood incidents (Dawson et al., 2011), seismic events (Liu et al., 2012), tsunamis (Wang et al., 2016), and hurricanes (Yin et al., 2014).

Our work introduces an agent-based building evacuation model defined on a continuous space. When evacuating a building, the agents select a global path, which corresponds to the fastest route from their current position to the exits of the building, using a shortest path algorithm (Dijkstra, 1959). At each time step, agents physically move like a particle flowing into a new position in the feasible domain following their global path, found by a constrained optimization problem of a predefined objective function (Van Den Berg et al., 2011). The logic of the motion includes very specific details such as physical collision avoidance among agents in order to model congestion (Van Den Berg et al., 2011).

This work uses the 08-A drill to validate the model with the observed evacuation of the K-12 school located a few meters away from the shoreline. The paper describes first the conceptual framework of the agent-based model used to simulate the evacuation process of the school. It then shows the building setting, the instrumentation and monitoring process of the drill, and the analysis of the data collected during the drill. Results of the drill in terms of velocities and flow rates are used to validate the proposed model. Finally, parametric simulations using the developed model are used to evaluate the impact of different values adopted by the physical parameters.

## 2. Methodology

### 2.1. Evacuation model

The model proposed herein to simulate building evacuations is described graphically in Fig. 1. The displacement of agents in space is modeled as an optimization problem at two different scales, defined as global path finding and local collision avoidance. First, each agent selects a global escape route that minimizes its expected evacuation time. After all agents have selected their global path, their movement is altered to ensure that no local collisions happen with static obstacles and among agents. The results are used to update position and velocity of the agents. Local collision avoidance has the effect of lowering the speed of agents in congested areas, and also enables faster agents to overtake slower agents by deviating slightly from the straight line to their local objective. This may result in another path being shorter, especially in places where two or more routes have comparable lengths. Thus, the global path of each agent is reevaluated at each time step as shown in Fig. 1.

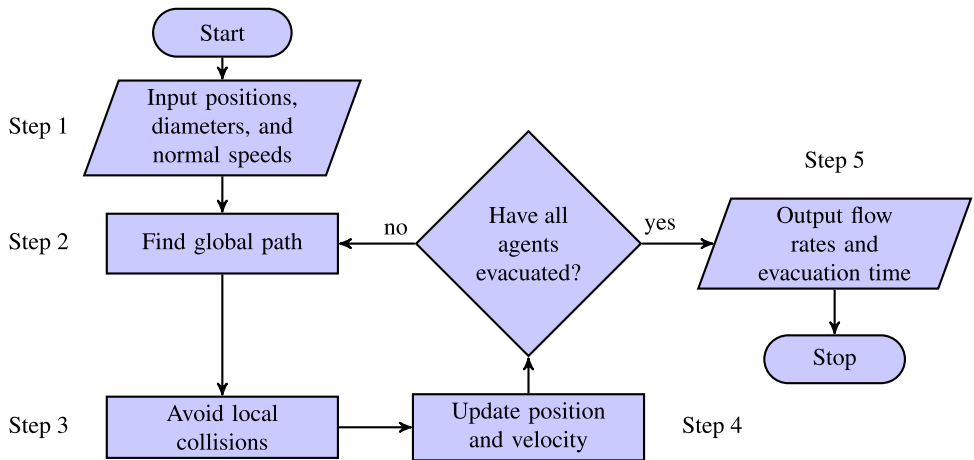


Figure 1: Flowchart of the human evacuation model.

#### 2.1.1. Personal attributes (Step 1)

Agents are assigned certain personal attributes in the model to be able to model realistic behaviors of heterogeneous populations, such normal speed and diameter (plan view). Age is an important variables to properly estimate the normal speed of the agent (Helbing et al., 2002). To enable the simulation of this effect, the proposed agent-based model separates young children in ages 4-6 from the rest of the population.

The normal agent speed is defined as the unimpeded walking speed,  $X$ , on a horizontal surface. It is assumed to be distributed among people as a Weibull distribution

$$f_X(x) = \frac{\alpha}{\beta^\alpha} x^{\alpha-1} e^{-(x/\beta)^\alpha}, \quad x \geq 0, \quad E[X] = \beta \Gamma\left(1 + \frac{1}{\alpha}\right) \quad (1)$$

where  $\alpha$  and  $\beta$  are the shape and scale parameter of the distribution, respectively; and  $\Gamma$  is the gamma function. The parameters of the distributions that were selected for this study are shown in Table 1. For adults and children of ages 7 and higher, the mean of the distribution is 1.34 m/s (Rinne et al., 2010), which is consistent with other sources (Fujiyama and Tyler, 2004; Proulx, 2002; Meister, 2007). The average speed of the distribution used for young children is 0.85 m/s, which was the mean speed observed by Larusdottir and Dederichs (2011). In this model, gender will not be considered in the selection of normal speed because there is no clear evidence of differences (Browning et al., 2006). Also, the unimpeded projected speed of agents using a stairway is reduced by 50% (Fujiyama and Tyler, 2004; Meister, 2007).

Table 1: Human speed parameters for a Weibull distribution.

Random variable	$\alpha$	$\beta$	Mean
adult normal speed	10.14	1.41	1.34 m/s
young children normal speed	3.80	0.94	0.85 m/s

Since people have bodies with a specific finite dimension, the model must ensure that all agents as they move neither overlap with other agents nor with the physical environment (e.g., partition walls and furniture). This is done by assigning to every agent a personal space around it that cannot be occupied by other agents, which is assumed in the model to be a circle in horizontal projection. This diameter was initially set as 45 cm, but a parametric analysis was performed to study the impact of this variable on the results.

### 2.1.2. Global path finding (Step 2)

There are several methodologies available to guide the selection of global routes in emergency evacuations (Løvås, 1998). The model presented here, uses an optimistic approach to find the global path of each agent, which assumes that each agent chooses the shortest path from their current position to the exits of the building. To visualize this goal-oriented behavior, consider an agent positioned at a starting point  $p_i$  with the goal of reaching point  $p_f$  (Fig. 2a). To reach its goal, the agent must navigate through the building avoiding static obstacles (e.g., walls and furniture), which can be thought of those having a polygonal shaded shape in the figure. The following definition states what the shortest path is, from a mathematical point of view:

**Definition 1.** *Let  $\mathcal{O}$  be a set of disjoint polygonal obstacles, and let  $p_i$  and  $p_f$  be two points that are not contained in  $\mathcal{O}$ . Then the shortest path between  $p_i$  and  $p_f$  is the shortest curve with endpoints in  $p_i$  and  $p_f$ , which does not intersect the interior of any polygon in  $\mathcal{O}$ .*

The shortest path can be shown to be a sequence of straight line segments connecting the vertices of the obstacles (Fig. 2a), as stated formally by the following Lemma, proven elsewhere (De Berg et al., 2008):

**Lemma 1.** *The shortest path between any two points  $p_i$  and  $p_f$  among a set  $\mathcal{O}$  of disjoint polygonal obstacles is a polygonal path whose inner vertices are convex vertices of  $\mathcal{O}$ .*

This result is important since it shows that from all the geometries found in a building, the agents will only use the convex vertices of the obstacles (i.e., vertices in which the internal angle of the polygon is less than  $180^\circ$ ) for their global path. Using this result, the building environment is transformed into a visibility graph (roadmap), which is used to navigate around static obstacles, as shown in the simple example of Fig. 2b. The example shows a building with two stories, a staircase, and one global exit. Each exit, staircase, and convex corner of an obstacle is a vertex of the graph. Since the agents have finite size bodies, they cannot reach the corner of an obstacle exactly, so the vertices are displaced by the radius of one agent in the direction of the bisector of the vertex’s angle. The edges (arcs) of the graph exist between vertices that can see each other, that is, if a straight line joining the vertices does not intersect the interior of any obstacle.

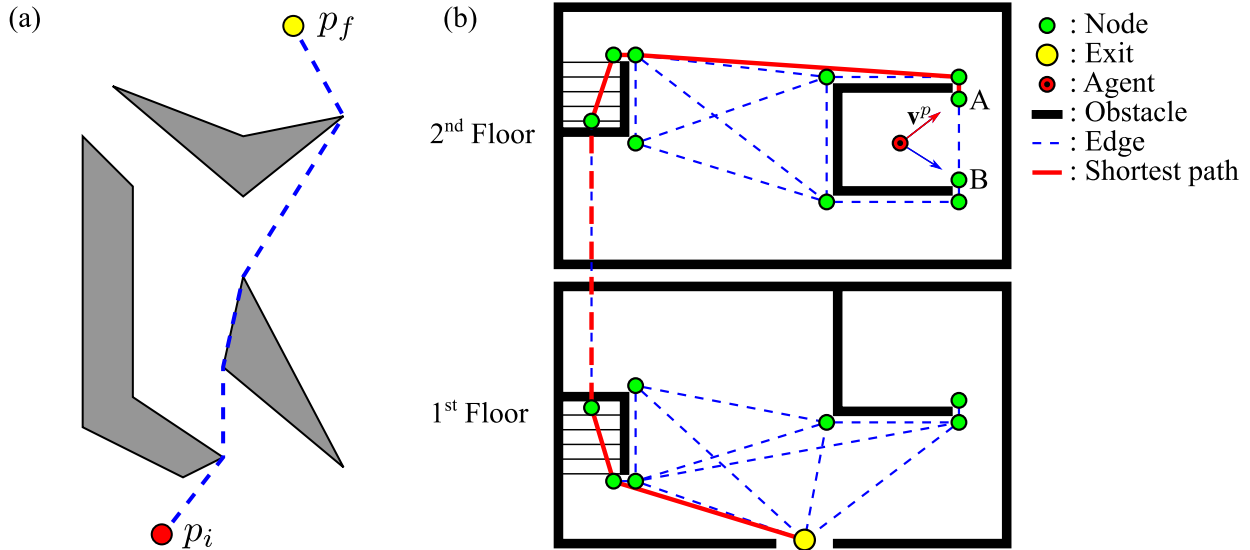


Figure 2: Agent navigation. (a) Shortest path between the current position,  $p_i$ , of an agent and its goal point,  $p_f$ . (b) Floor plan of a simple two story building and its transformation into a visibility graph.

The weight (cost) of each edge is set as the distance between the two vertices at the end of the edge. This visibility graph can be computed efficiently in  $O(m^2)$  time (Asano et al., 1986), where  $m$  is the total number of edges in the polygons.

The shortest path from each vertex  $j$  to the exits of the building is then computed using Dijkstra's algorithm (Dijkstra, 1959), and the length of the path is  $d_j$ . This process is done only once prior to the start of the simulations. Since all vertices of the graph must be visited in this precomputation step, there is no advantage in using A\* heuristics. At every time step, the global path of each agent  $i$  is found by selecting from the vertices that the agent can see, the one that minimizes the distance to get to an exit:

$$c_i = \arg \min_{j \in \mathcal{S}_i} (d_j + \|\mathbf{r}_i - \mathbf{r}^j\|), \quad \forall i \in \mathcal{N} \quad (2)$$

where  $d_j$  is the shortest distance from vertex  $j$  to the building exits;  $\mathbf{r}_i$  is the position of agent  $i$ ;  $\mathbf{r}^j$  is the position of vertex  $j$ ;  $\mathcal{S}_i$  is the set of all the vertices visible to agent  $i$ ;  $\mathcal{N}$  is the set of the agents that are evacuating the building; and  $\|\cdot\|$  denotes the Euclidean norm. In the example of Fig. 2b, the agent (red circle) can only see vertices A and B, and chooses A because it minimizes the distance to the exit. The preferred velocity of the  $i$ -th agent is then constructed as a vector pointing to the vertex  $c_i$  that minimizes the time to get to the exits

$$\mathbf{v}_i^p = \frac{(\mathbf{r}^{c_i} - \mathbf{r}_i)}{\|\mathbf{r}^{c_i} - \mathbf{r}_i\|} v_i^n f_i, \quad \forall i \in \mathcal{N} \quad (3)$$

where  $\mathbf{r}^{c_i}$  is the position of vertex  $c_i$ ;  $v_i^n$  is the normal speed of agent  $i$ ; and  $f_i$  is a correction factor which reduces from 1 to 0.5 in staircases (Fujiyama and Tyler, 2004; Meister, 2007).

### 2.1.3. Local collision avoidance (Step 3)

After all the preferred velocities of the agents have been computed, they must be adjusted to ensure there is no collision with static obstacles and amongst agents. This is accomplished by using the Optimal Reciprocal Collision Avoidance principle (ORCA) (Van Den Berg et al., 2011), which implies that each agent selects independently and simultaneously a new velocity  $\mathbf{v}_i^n$  that is as near as possible to its preferred velocity, but avoids collisions with stationary obstacles and other agents, i.e.

$$\mathbf{v}_i^n = \arg \min_{\mathbf{v} \in \mathcal{V}_i^\tau} \|\mathbf{v} - \mathbf{v}_i^p\|, \quad \forall i \in \mathcal{N} \quad (4)$$

where  $\mathcal{V}_i^\tau$  is the set of all possible velocities that ensure that agent  $i$  will not collide for at least a time window of  $\tau$ . Set  $\mathcal{V}_i^\tau$  is explained in detail by Van Den Berg et al. (2011), and consists of the intersection of half-planes

of permitted velocity. Each of these constraints represents collision avoidance with an agent or static obstacle that is nearby, and is constructed assuming that agents observe the current position, velocity, and diameter of the other agents around it. For collision avoidance between agents, the algorithm assumes that agents will share the responsibility of collision avoidance and use the same strategy to select their new velocities. In the case of static obstacles, agents take full responsibility of the collision avoidance. The number of half-plane constraints increases with agent density and decreases the selected speeds obtained from the optimization process, resulting in the emergence of congestion.

The new position of an agent  $\mathbf{r}_i^n$  is then computed using the calculated velocity

$$\mathbf{r}_i^n = \mathbf{r}_i + \mathbf{v}_i^n \Delta t \quad , \forall i \in \mathcal{N} \quad (5)$$

where  $\mathbf{r}_i$  represents in Eq. (5) the position of the  $i$ -th agent in the previous time instant, and  $\Delta t$  is the model's time step, which is chosen as 0.05 s.

The pseudo Algorithm 1 summarizes how the movement of the agents is modeled in this study. The algorithm is written in pseudocode and is self-explanatory. The shortest paths of the visibility graph are constructed only once, and before the simulation starts. At each time step, the preferred velocities of an agent are computed, and adjusted to ensure that there are no collisions with physical obstacles or between agents. Finally the positions and velocities of the agents are updated.

---

**Algorithm 1:** Pseudocode for calculating the motion of agents.

---

**Data:** Set the following parameters

$n$ : number of initial agents;  $\Delta t$ : time step;  $n_{sim}$ : number of simulations

**begin**

Construct the vertex set  $V$ , which includes all exits, stairs, and convex corners of obstacles;

Construct the edge set  $E$ , defined by the visibility among vertices in  $V$ ;

Form the visibility graph  $G = (V, E)$  where the weights associated with the edges are defined by the distance among vertices;

Use Dijkstra's algorithm (Dijkstra, 1959) to find the minimum distance  $d_j$  from each vertex  $j \in V$  to the exits of the building;

**for**  $k \leftarrow 1$  **to**  $n_{sim}$  **do**

Create  $n$  agents, where  $\mathcal{N}$  is the set of all agents;

Position each agent  $i \in \mathcal{N}$  at a point  $\mathbf{r}_i$  in the building plan, and set its initial velocity to

$\mathbf{v}_i \leftarrow \mathbf{0}$ ;

**while**  $|\mathcal{N}| > 0$  (*not all agents have evacuated*) **do**

**for**  $i \in \mathcal{N}$  **do**

Find the set of vertices  $\mathcal{S}_i$  visible to the  $i$ -th agent;

Select vertex  $c_i$  followed by the  $i$ -th agent according to Eq. (2);

Set the preferred velocity  $\mathbf{v}_i^p$  of the  $i$ -th agent using Eq. (3);

Construct the set  $\mathcal{V}_i^r$ , consisting of all feasible velocities of the  $i$ -th agent;

Compute the new velocity  $\mathbf{v}_i^n$  of the  $i$ -th agent using Eq. (4);

**end**

**for**  $i \in \mathcal{N}$  **do**

Update the position:  $\mathbf{r}_i \leftarrow \mathbf{r}_i + \mathbf{v}_i^n \Delta t$ ;

Update the velocity:  $\mathbf{v}_i \leftarrow \mathbf{v}_i^n$ ;

**end**

Remove from  $\mathcal{N}$  the agents that have evacuated through an exit;

Update time by  $\Delta t$ ;

**end**

**end**

**end**

---

## 2.2. Case study

An evacuation drill of a K-12 school (Colegio Inglés) in Iquique, Chile, was chosen as a testbed to validate the model just presented. The school is located at 70 meters from the shoreline as shown in Fig. 3c, which makes it extremely vulnerable to inundation due to a tsunami. One of the benefits of selecting a school as a testbed is that most agent attributes, say age and location at the beginning of the evacuation drill, are known for most occupants. This information reduces uncertainty in the model parameters and enables us to better establish the epistemic uncertainty associated with the model by comparing its results with measured data from the drill.



Figure 3: K-12 school where the drill was performed, and its location in Iquique. (a) Kingswood building. (b) Partially blocked school exit E2. (c) Evacuation map of Iquique with evacuation routes (red lines) and safety zones (green dots).

The drill took place August 8<sup>th</sup>, 2013 as part of a planned earthquake and tsunami drill in the coastline of the four northern regions of Chile. It was organized by the Chilean National Emergency Office (ONEMI), which depends on the Ministry of Interior and Public Security. About 267,000 people participated in this evacuation, of which 76,000 were from the city of Iquique and evacuated from the coastline along specified routes (red lines) to the safety zones shown in Fig. 3c (green dots). The expected outcomes of this drill were to continue to promote a culture of preparedness in the population, train them for future events (e.g., April 1<sup>st</sup> 2014), and evaluate the evacuation times required to reach the safety zones (Walker, 2013). The staff and students of the school, which were a total of 1545, knew that a tsunami drill was going to take place that day in the city, but they did not know the exact starting time. The tsunami sirens of the city went off at approximately 11:28 AM.

The school has five buildings as shown schematically in Fig. 4. Only four of the five buildings were being used when the drill started; one of them shown in Fig. 3a. During drills or real events only two exits of

the school are used to evacuate, denoted as E1 and E2. Herein, the stairways are named with the initial of the building they belong to; and they run on the exterior of the building connecting upper stories to the schoolyard. The evacuation drill was monitored using twenty-five digital video cameras that remained stationary, of which six were security cameras that are permanently installed in the buildings of the school. The layout of some of the most important cameras and their lines-of-sight are shown in Fig. 4.

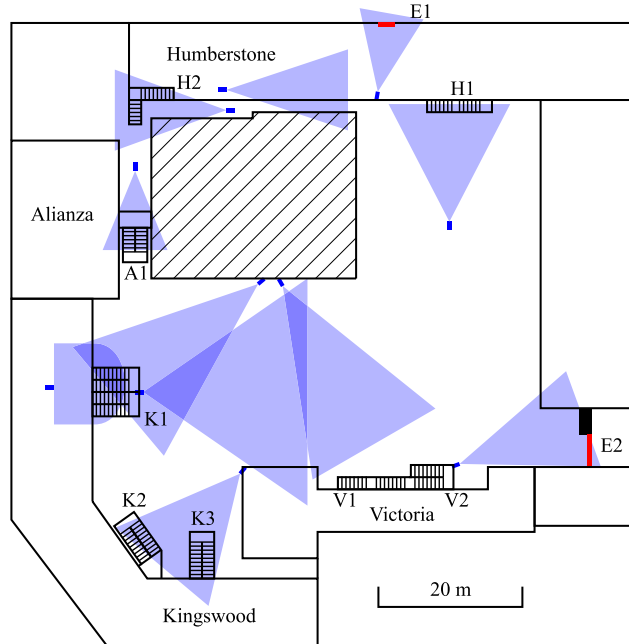


Figure 4: Plan view of the school, building and exit denominations, and camera layout.

To simulate the effect of earthquake damage, in which structural or non-structural elements could fall down during an earthquake, five physical interventions were set up before the evacuation drill. These physical interventions were: (1) fallen 3x4 m soccer goal in schoolyard; (2) blocked staircase in Kingswood building; (3) partially blocked passageway in Humberstone building; and (4) partially blocked exit E2, shown in Fig. 3b. All interventions were included in the model simulations as physical obstacles. Furthermore, students of six classes were chosen to wear T-shirts of different colors to observe patterns of group behavior. These were split in two classes of kindergarten, fifth grade, and ninth grade.

### 3. Results and Discussion

In each classroom, the time between the start of the drill and the start of their evacuation process (pre-evacuation time) was measured and is presented in Fig. 5. This figure also shows the cumulative distribution function (CDF) and probability density function (PDF) of the time lag. A Weibull distribution was fitted to the data, which was computed using the maximum likelihood method (Hoel, 1962). It took about 110 seconds for everyone to start evacuating and the model fit looks quite reasonable.

The agent-based model described in the previous section was implemented in Netlogo (Wilensky, 1999), a multi-agent programmable modeling environment, mainly due to its good compatibility with models of agents interacting locally and its excellent documentation relative to other ABM environments (Railsback et al., 2006). The floor plans of the school were not available and had to be reconstructed using a laser scanning technology. Each of the buildings were then transformed into two dimensional maps with the following component types: wall, stair, exit, and floor. Staircases are used to connect nonadjacent points of the grid by transporting agents in elevation in order to emulate the real 3D environment. The actual stair space is modeled in the same two dimensional space as a floor with reduced speed.

The number and age of the students that were in each classroom when the drill started were known. However, the starting position of each person inside the classrooms was assigned randomly. For each class,

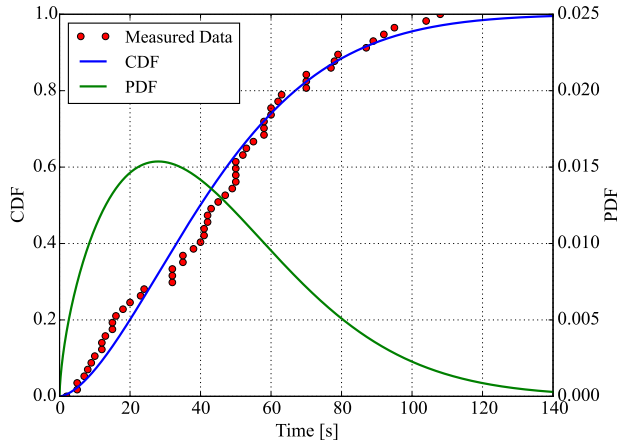


Figure 5: Pre-evacuation times of the different classes of the school and the CDF (blue) and PDF (green) of the fitted Weibull distribution with parameters  $\alpha = 1.634$  (shape) and  $\beta = 49.96$  (scale).

the pre-evacuation time was adjusted to match the observed data obtained from the videos. The agents representing students and staff not located inside classrooms at the start of the drill, were distributed in common areas based on the video recordings; the distribution fitted in Fig. 5 was used to select their individual pre-evacuation times. The four buildings of the school were modeled independently. The outputs of each building were used as inputs of another model representing the school grounds.

Table 2 shows the number of vertices and edges of the visibility graph that was generated for each school building to compute shortest paths. It also presents the running times of visibility graph generation, Dijkstra’s algorithm, other precomputations, and evacuation simulation, as a percentage of the total running time of the model. Almost all the computation time was spent in the evacuation simulation, which is mainly used to compute the vertices that each agent can see and perform collision avoidance. All precomputation steps, including visibility graph generation and Dijkstra’s algorithm, use a very small fraction of the computation time. Other kinds of graphs generation techniques for buildings exist that can result in simpler networks with less vertices and edges (e.g., Chen and Huang, 2015). These graphs are generally faster to construct and analyze, but do not guarantee the selection of the shortest route to exit the building. However, for the buildings considered in this study the construction and use of the visibility graphs took less than 0.3% of the total simulation time, and hence visibility graphs were deemed the best choice for selecting shortest paths in the model.

Table 2: Visibility graph properties and relative running times for each building.

Building	Visibility graph properties		Running times (%)			
	# of vertices	# of edges	Visibility graph	Dijkstra’s algo.	Other precomp.	Evacuation
Humberstone	168	3244	0.27	0.019	1.59	98.1
Alianza	114	1176	0.24	0.051	1.27	98.4
Kingswood	200	2188	0.16	0.064	0.80	99.0
Victoria	67	620	0.22	0.046	1.04	98.7

As an example, Fig. 6 shows a simulation of the Victoria building at four different time instants ( $t = 0, 20, 40,$  and  $60$  s). At first, all the children (red dots) are inside their classrooms. The frame at  $t = 20$  s shows only one class starting to evacuate, and the frame at  $t = 40$  s shows all of the classes evacuating. In the final frame at  $t = 60$  s all of the students are in the staircase area and the building simulation is essentially over when they descend to the ground floor.

The numerical model and the real evacuation were compared using the so-called evacuation curves, which represent the cumulative number of evacuated people as a function of time. Thus, Fig. 7 compares the evacuation curves obtained by 25 simulations of the drill model of the four buildings. The errors observed between simulations and measured data are quite small. Mean, maximum, and minimum errors in predicting

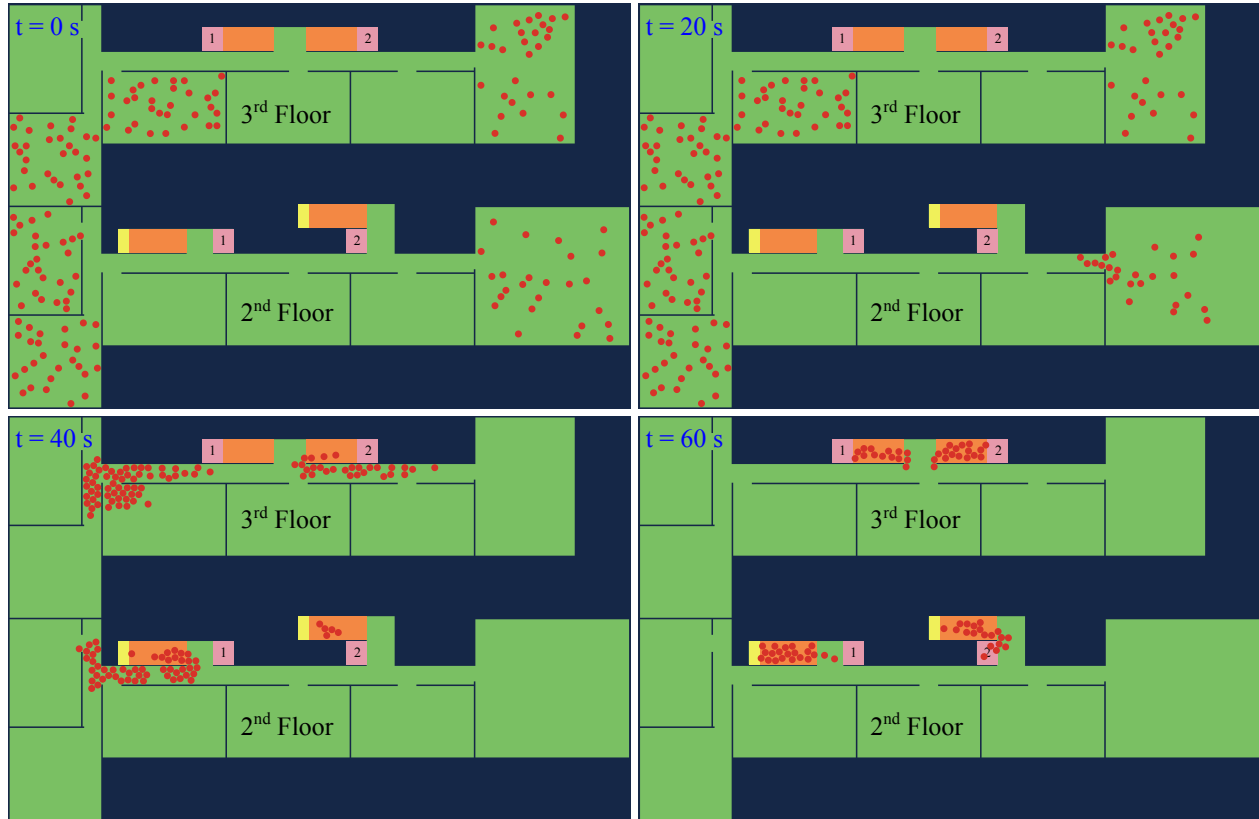


Figure 6: Snapshots of one evacuation simulation of the Victoria building at times  $t = 0, 20, 40,$  and  $60$  s.

the complete evacuation time  $t_f$  are included in each plot. It is apparent that the simulations have little variability among them; such is the case because the classrooms where each person was located are known. Obviously, this variability would increase in cases where the initial conditions of agent location are uncertain. It is also worth mentioning that these curves were not adjusted to match the measured response, which is very positive in terms of the predictability and robustness of the agent-based model. Furthermore, the time required to evacuate each building varies significantly due to the specific building layout and occupancy, which validates the need for the modeling of each building as a different unit.

Table 3 summarizes several indicators of the flow of people through the control points, i.e. each of the eight stairways and the two school exits (Fig. 4). It presents an empirical flow rate determined as the slope of a least squares straight line fitting the measured evacuation curve. In this table, the estimated flow rate is divided by the width of the section to obtain a normalized flow rate, which enables comparison of pathways with different widths. There are several interesting results to highlight based on the data from Table 3. First, that in spite of the complexity of the phenomenon, the estimates of the normalized rate obtained by the agent-based model are quite reasonable. Indeed the average errors in staircases and exits are 16.2% and 2.7%, respectively. However, the staircases with the largest errors are the ones where the model cannot predict correctly the number of people that use them (e.g., Kingswood and Victoria buildings). This error of prediction occurs when there are classrooms that have two or more alternative escape routes with similar distances. The model chooses analytically the shortest route for each agent inside the classroom, but people cannot discriminate small differences in distance and randomly choose any of the routes. Second, the variability among normalized flow rates in staircases is characterized by a range of [1.25-2.07] P/s/m, which is quite significant. Such variation is determined by the density and speed of people in each staircase, with the maximum capacity being achieved at staircases with normalized flow rates of around 2 P/s/m. For the case of the exits they both showed dissimilar normalized flow rates ranging from [1.45-3.24] P/s/m. Exit E1 showed high congestion and was probably at its maximum capacity with a normalized flow rate of 3.24 P/s/m, which is close to the average values of 3.2 P/s/m obtained experimentally by Daamen and Hoogendoorn (2012)

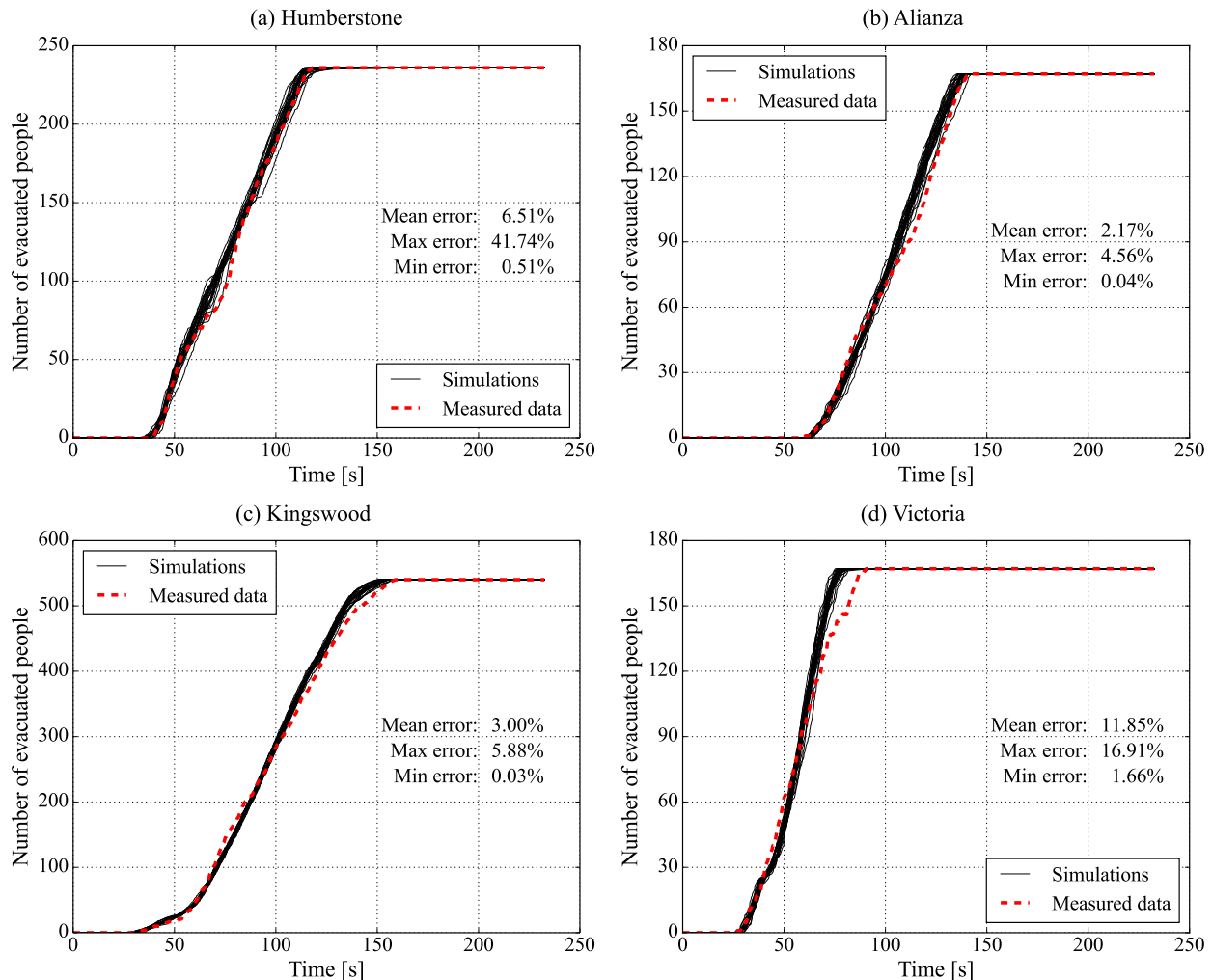


Figure 7: Comparison of the evacuation history of the experiment and the model for each building.

with the population of a school. This same study found schools to be the facilities with the greatest flow rate since their occupants are mostly children and have smaller sizes than adults and hence tend to maximize the capacity of a congested exit (Daamen and Hoogendoorn, 2012). Exit E2 had a smaller normalized flow rate due to its large width, which precluded congestion.

Fig. 8 shows the same comparison as done for Fig. 7 for the two exits of the school. Both exits are then summed to obtain the total evacuation curve for this school. In general, experimental results show that people tend to evacuate faster than the model predicted, but the results match very well after 150 s at the east exit (E2), and after 100 s at the north exit (E1). The accuracy presented by the model developed is deemed sufficient for the design of new interventions in the school to improve the total time required to evacuate. The curve of total cumulative shows the same trend as the east exit (E2).

A general summary of the geometric properties of each of the four buildings of the school are shown in Table 4, together with the number of people who were inside at the beginning of the drill, and the time required for the first and last person to evacuate, denoted as  $t_i$  and  $t_f$ , respectively. Numbers for each building correspond to the sum of all staircases and do not include children in the classrooms on the first floor since doors open directly into the schoolyard. Table 4 also shows the total number of people that evacuated the school, which considers: all the staircases, the first floor of the four buildings, and people that were in the schoolyard when the evacuation drill started.

Some results of Table 4 are also worth commenting. As it was previously stated, the model seems to predict quite well the measured results. Average errors for the four buildings and the complete school are

Table 3: Summary of data obtained at each stair and school exit, normalized flow rates (in person per second per meter [P/s/m]), and number of people that crossed each control section.

Section	Flow rate [P/s]	Width [m]	Norm. rate [P/s/m]			# of people		
			Drill	Model	Error [%]	Drill	Model	Error [%]
Stair H1	3.04	1.47	2.07	2.11	1.9	145	145	0.0
Stair H2	2.49	1.30	1.92	2.06	7.3	91	91	0.0
Stair A1	2.15	1.40	1.54	1.76	14.3	167	167	0.0
Stair K1	2.27	1.29	1.76	1.52	13.6	207	172	17.0
Stair K2	1.63	1.30	1.25	1.65	32.0	115	163	41.7
Stair K3	2.38	1.25	1.91	2.06	7.9	218	205	6.0
Stair V1	2.12	1.43	1.48	2.01	35.8	82	97	18.3
Stair V2	1.92	1.39	1.38	1.61	16.7	85	70	17.6
Exit E1	6.80	2.10	3.24	3.35	3.4	536	534	0.4
Exit E2	6.38	4.40	1.45	1.42	2.1	1009	1011	0.2

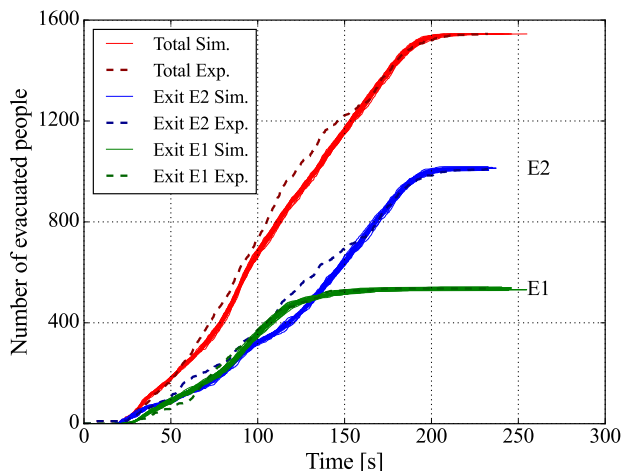


Figure 8: Comparison of the evacuation history of the experiment (dashed lines) and the simulations of the model (solid lines) for both exits and the complete school (aggregated results from E1 and E2).

5.9% and 1.0%, respectively. In general, accuracy in the aggregated results for the staircases and the global school are always smaller than for specific staircases. Also, predicted times  $t_i$  and  $t_f$  are quite accurate, which is expected for  $t_i$  but not necessarily for  $t_f$ , which again shows the reasonable fit of the agent-based model relative to reality. Evacuation times of staircases fluctuated between slightly above 1 minute to about 2 minutes. Evacuation time for the whole school was about 3.5 minutes.

A parametric analysis was carried out to study the sensitivity of two physical parameters of the model: the normal speeds of agents, and their diameters. The effect of these two parameters is analyzed using an error measure. The error  $D(\theta)$  is calculated as the area between the evacuation curve of the drill and the average evacuation curve obtained from the simulations:

$$D(\theta) = \int_0^{t_f} |p_m(t, \theta) - p_d(t)| dt \quad (6)$$

where  $\theta$  is the selected value of the parameter;  $p_d(t)$  is the evacuation curve of the drill;  $p_m(t, \theta)$  is the predicted evacuation curve using the model (average of all the simulations); and  $t_f$  is the time when the last person evacuated the premises of the school in the drill. The impact that a parameter has on the goodness of the prediction will be quantified by a normalized error, which is obtained by dividing the error value of

Table 4: Geometrical and evacuation data of each building of the school.

Building	N° of floors	Area/floor [m <sup>2</sup> ]	N° of people	$t_i$		$t_f$		Error [%]
				Drill	Model	Drill	Model	
Humberstone	3	754	236	0:39	0:39	1:58	2:06	6.5
Alianza	3	331	167	1:00	1:04	2:22	2:18	2.2
Kingswood	4	766	540	0:31	0:32	2:39	2:34	3.0
Victoria	3	210	167	0:27	0:30	1:31	1:20	11.8
Complete School	-	-	1545	0:06	0:20	3:51	3:49	1.0

Eq. (6) by the same error obtained assuming the initial (nominal) value  $\theta_0$  of the parameter:

$$\hat{\epsilon}(\theta) = \frac{D(\theta)}{D(\theta_0)} \quad (7)$$

The normalized error,  $\hat{\epsilon}(\theta)$ , corresponding to the simulations of each building and the complete school as a function of different values of the normal agent speed and agent diameter are presented in Figs 9a and 9b, respectively. Black circles in the figure represent the initial values  $\theta_0$  of the parameters, which, by construction, have a normalized error of 1. The normal speed parameter  $\bar{v}$  corresponds to the mean of the normal speed distribution for adults shown in Table 1. The normal speed of each agent, which was sampled from one of the distributions, was multiplied by the ratio between the new mean value  $\bar{v}$  and the original value of 1.34 m/s. It is apparent that the initial values selected of 1.34 m/s for the mean of the normal speed distribution  $\bar{v}$  and 45 cm for the agent diameter  $d$ , used in the simulations are close to the speed and diameter that produces minimum error in all structures. The normal speed that minimizes the error for the complete school is approximately 0.2 m/s higher than the speed for each building independently, which suggests that the model should assume higher speeds for the agents in open spaces than inside buildings. As for the diameter of agents, results show that the model is more sensitive to an increase in this parameter above the optimal value than to a decrease in it. This is because for small diameters agent congestion decreases and the evacuation is controlled by the normal speed of agents, while an increase in diameter generates congestion, which significantly affects the evacuation time. For three of the four buildings the variation shown relative to the parameter is quite significant, which shows the importance and sensitivity of the response relative to these parameters.

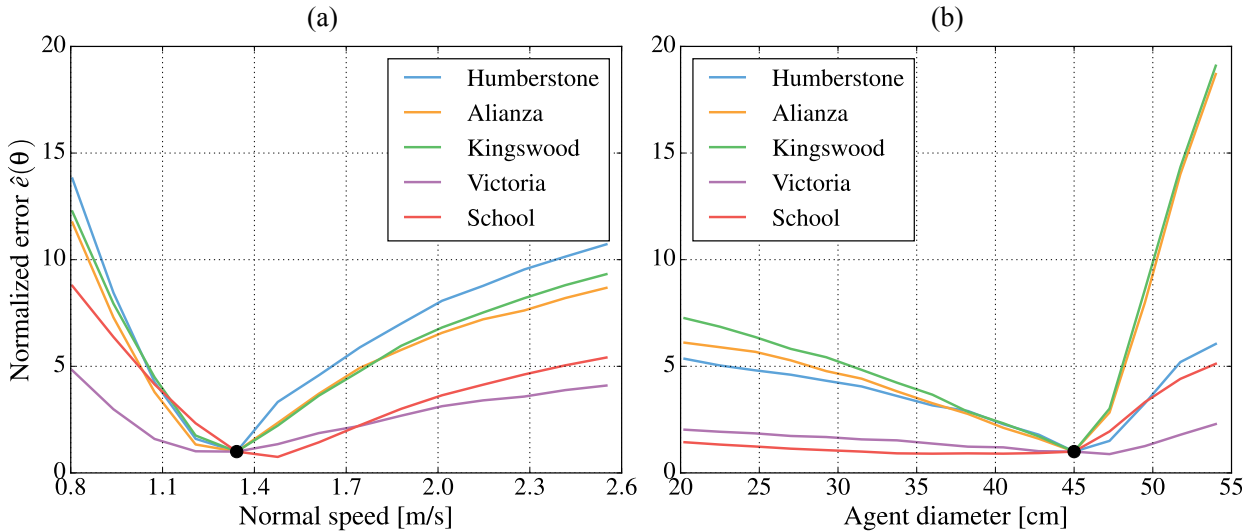


Figure 9: Normalized error  $\hat{\epsilon}(\theta)$  of the simulations for different values of (a) Normal speed  $\bar{v}$ , and (b) Agents diameter  $d$ .

## 4. Conclusions

This research describes the development of an agent-based model aimed at simulating human evacuation processes. The model parameters were validated with real data from an evacuation drill of a K-12 school in the city of Iquique, Chile. Differences between results of the simulations and the actual drill are relatively small with an average error in the evacuation time of 5.9% for the four buildings and 1.0% for the complete school. The average error of the flow rates in stairs and exits is slightly larger and reaches 13.5%. The time required to evacuate the 1545 students out of the school premises was 3.85 minutes and the complete evacuation to the safety zone (30 m height) took approximately 18 minutes. The normalized flow rates of agents in the staircases range from 1.38 to 2.07 persons per second per meter, and agent velocities obtained during the drill are quite comparable with data available previously in the literature.

The quality of the simulation estimations is affected by several parameters that must be defined before the simulation starts, such as the starting time and position, normal velocities, and diameter of agents. These parameters affect the flow and congestion of evacuation routes, and hence the overall evacuation time. The good agreement between the model and the drill is probably due to the low uncertainty of these parameters for the particular case study. However, since model parameters are rarely known in practice, a sensitivity analysis was carried out for two of them. The parametric analysis conducted shows that normal velocities of agents and the diameter of agents play an important role in the estimation of the evacuation times. The research showed that the effect of these parameters is highly non-linear and the agent-based model is capable of capturing this non-linearity. This implies that slight perturbations of the nominal values leads to significant changes in evacuation time. All the results obtained from the drill suggest that the model can also be used as a predictive tool for human evacuation in buildings triggered by different hazards (e.g., earthquakes, tsunamis, and fires). Consequently, possible future applications of this tool are to generate simulation based optimal evacuation plans. Furthermore, building evacuation routes are usually designed following safety codes that provide minimum requirements, such as minimum stair widths and maximum route lengths, but do not estimate the real performance of the design. The proposed model solves this limitation, and can therefore be used to assess the effectiveness of different building escape layouts before its construction and provide valuable information on where possible bottlenecks could occur.

Almost all of the people who participated in the school drill had a very good knowledge of their surrounding physical environment since they attend school daily. This resulted in an efficient evacuation with evacuees having a clear route to exit the school. Thus, the assumptions used by the model to simulate agent movement, i.e. that every agent chooses the shortest path to an exit and that their selected velocity follows this path as close as possible while avoiding other agents and obstacles, are not far from reality. Such is not the case for some other buildings occupied by less informed people, say shopping centers or stadiums, of which they only have partial information of the geometry, such as the path they used to enter. A simplified way to model this case is to find the shortest path from each of the building exits to all the vertices of the visibility graph, and have agents choose the routes that go only to exits that they know.

Another issue related to the selection of shortest paths is their invariance relative to the density of agents using them. This limitation can be addressed by changing the costs of edges in the visibility graph, initially set as the distance between nodes, to a time-dependent travel time estimated with the speed of agents using each edge (e.g., Asano et al., 2010). Thus, though some agents would select sub-optimal paths in terms of length, they would still minimize their estimated travel time to the final goal by accounting for congestion.

The model used in this study does not include social behaviors beyond the physical interactions derived from the local collision avoidance algorithm. Empirical evidence from evacuation drills and real fire alarms (Jones and Hewitt, 1986; Rinne et al., 2010) have shown that agents may transfer knowledge, group, imitate behaviors of others, and present a number of other social behaviors that affect their decisions to move within a building. These behaviors have been included in several evacuation models (e.g., Yang et al., 2005; Gwynne et al., 2006; Pan et al., 2007; Lu et al., 2017), normally without a detailed description of their implementation. However, the modeling of these phenomena is not straightforward and the hard data required to back up these behaviors are very scarce or simply nonexistent in the literature, so models typically rely on strong assumptions based on the opinion of experts rather than empirical data. The good agreement shown in our case between the experimental and simulated evacuation suggests that apparently for this particular drill the effect of social behaviors was not relevant, probably due to the fact that students knew well the school infrastructure, their classmates, and the drill procedures, and hence, did not need to resource to these social behaviors to evacuate. Future works could study how these social behaviors affect the evacuations and see

if they improve the results when compared with experimental data. This could be especially important for other types of buildings where the occupants are less familiar with the physical environment around them or have not participated in a drill.

Despite the accurate predictions obtained by the model, the decision of agents when choosing between two alternative and comparable routes from the point of view of minimizing the evacuation time objective function may lead to an important source of model error. Perhaps a questionnaire of people's daily use of staircases could resolve this and be added to the agents behavior repertoire, as has been done previously for exit selection (Duives and Mahmassani, 2012). However, this issue still requires further research to discover better rules to define the motion of agents, capable of modeling these apparently indifferent decisions. Furthermore, the accuracy of the model may well be a result of the particular case of this school where the location and pre-evacuation time of most of the people at the start of the drill was known. This also requires further study to validate the robustness of blind predictions, since this information is unavailable in predicting future evacuations where the number and distribution of occupants at the time of the event is unknown. However, it is relevant to emphasize that the main objective of this work was precisely to understand the quality of ABM in terms of its predictive capacity if all variables were controlled.

Future stages of this research will also address the modeling of larger evacuation processes at a block and city scale due to possible inundation, and affected by debris due to possible damage or total collapse of structures and their components. Empirical data of other evacuation behaviors from recent events in Chile will be used to improve the estimation of casualties, injuries, and loss of other social variables needed to predict the response of communities subjected to extreme events.

## Acknowledgments

This study was supported financially by the National Research Center for Integrated Natural Disaster Management CONICYT/FONDAP/15110017, and by Fondecyt [grant numbers 1141187, 1170836], from the Chilean National Commission for Scientific and Technological Research (CONICYT). The authors also thank the company GEOCOM for performing the laser scan of the school and the Colegio Inglés of Iquique for their support in obtaining data from the evacuation drill.

## References

- Arthur, W.B., 2006. Out-of-equilibrium economics and agent-based modeling. *Handbook of computational economics* 2, 1551–1564.
- Asano, M., Iryo, T., Kuwahara, M., 2010. Microscopic pedestrian simulation model combined with a tactical model for route choice behaviour. *Transportation Research Part C: Emerging Technologies* 18, 842–855.
- Asano, T., Asano, T., Guibas, L., Hershberger, J., Imai, H., 1986. Visibility of disjoint polygons. *Algorithmica* 1, 49–63.
- Bonabeau, E., 2002. Agent-based modeling: Methods and techniques for simulating human systems. *Proceedings of the National Academy of Sciences of the United States of America* 99, 7280–7287.
- Browning, R.C., Baker, E.A., Herron, J.A., Kram, R., 2006. Effects of obesity and sex on the energetic cost and preferred speed of walking. *Journal of Applied Physiology* 100, 390–398.
- Catalán, P., Aránguiz, R., González, G., Tomita, T., Cienfuegos, R., González, J., Shrivastava, M.N., Kumagai, K., Mokrani, C., Cortés, P., et al., 2015. The 1 april 2014 pisagua tsunami: Observations and modeling. *Geophysical Research Letters* 42, 2918–2925.
- Chen, A.Y., Huang, T., 2015. Toward bim-enabled decision making for in-building response missions. *IEEE Transactions on Intelligent Transportation Systems* 16, 2765–2773.
- Chlieh, M., De Chabaliér, J., Ruegg, J., Armijo, R., Dmowska, R., Campos, J., Feigl, K., 2004. Crustal deformation and fault slip during the seismic cycle in the north chile subduction zone, from gps and insar observations. *Geophysical Journal International* 158, 695–711.

- Daamen, W., Hoogendoorn, S., 2012. Emergency door capacity: influence of door width, population composition and stress level. *Fire technology* 48, 55–71.
- Dawson, R.J., Peppe, R., Wang, M., 2011. An agent-based model for risk-based flood incident management. *Natural hazards* 59, 167–189.
- De Berg, M., Schwarzkopf, O.C., Van Kreveld, M., Overmars, M., 2008. *Computational geometry*. Third ed., Springer Berlin Heidelberg.
- Dijkstra, E.W., 1959. A note on two problems in connexion with graphs. *Numerische mathematik* 1, 269–271.
- Duives, D., Mahmassani, H., 2012. Exit choice decisions during pedestrian evacuations of buildings. *Transportation Research Record: Journal of the Transportation Research Board* 2316, 84–94.
- Fraser, S., Raby, A., Pomonis, A., Goda, K., Chian, S.C., Macabuag, J., Offord, M., Saito, K., Sammonds, P., 2013. Tsunami damage to coastal defences and buildings in the march 11th 2011 Mw9.0 great east japan earthquake and tsunamis. *Bulletin of Earthquake Engineering* 11, 205–239.
- Fujiyama, T., Tyler, N., 2004. Pedestrian speeds on stairs: an initial step for a simulation model, in: *Proceedings of 36th Universities Transport Studies Group Conference, Newcastle upon Tyne, UK*. pp. 7C1.1–11.
- Guha-Sapir, D., Below, R., Hoyois, P., 2016. EM-DAT: International disaster database. <http://www.emdat.be/database>. Accessed: May 2016.
- Gwynne, S., Galea, E.R., Lawrence, P.J., 2006. The introduction of social adaptation within evacuation modelling. *Fire and Materials* 30, 285–309.
- Helbing, D., 1992. A fluid-dynamic model for the movement of pedestrians. *Complex Systems* 6, 391–415.
- Helbing, D., Farkas, I., Vicsek, T., 2000. Simulating dynamical features of escape panic. *Nature* 407, 487–490.
- Helbing, D., Farkas, I.J., Molnar, P., Vicsek, T., 2002. Simulation of pedestrian crowds in normal and evacuation situations, in: Schreckenberg, M., Sharma, S.D. (Eds.), *Pedestrian and evacuation dynamics*. Springer, Berlin, pp. 21–58.
- Helbing, D., Isobe, M., Nagatani, T., Takimoto, K., 2003. Lattice gas simulation of experimentally studied evacuation dynamics. *Physical review E* 67, 067101.
- Helbing, D., Molnar, P., 1995. Social force model for pedestrian dynamics. *Physical review E* 51, 4282–4286.
- Henderson, L., 1971. The statistics of crowd fluids. *Nature* 229, 381–383.
- Hoel, P.G., 1962. *Introduction to mathematical statistics*. third ed.. John Wiley & Sons Inc. pp. 56–61.
- Hughes, R.L., 2002. A continuum theory for the flow of pedestrians. *Transportation Research Part B: Methodological* 36, 507–535.
- Jones, B.K., Hewitt, J.A., 1986. Leadership and group formation in high-rise building evacuations, in: *Fire Safety Science - Proceedings of the First International Symposium*. Hemisphere Publishing Corp., pp. 513–522.
- Lakoba, T.I., Kaup, D.J., Finkelstein, N.M., 2005. Modifications of the helbing-molnar-farkas-vicsek social force model for pedestrian evolution. *Simulation* 81, 339–352.
- Larusdottir, A.R., Dederichs, A., 2011. Evacuation dynamics of children—walking speeds, flows through doors in daycare centers, in: Peacock, R.D., Kuligowski, E.D., Averill, J.D. (Eds.), *Pedestrian and Evacuation Dynamics*. Springer, pp. 139–147.
- Lay, T., Yue, H., Brodsky, E.E., An, C., 2014. The 1 april 2014 iquique, chile, mw 8.1 earthquake rupture sequence. *Geophysical Research Letters* 41, 3818–3825.

- Liu, Z., Jalalpour, M., Jacques, C., Szyniszewski, S., Mitrani-Reiser, J., Guest, J., Igusa, T., Schafer, B., 2012. Interfacing building response with human behavior under seismic events, in: 15th World Conference on Earthquake Engineering, Lisbon, Portugal.
- Løvås, G.G., 1998. Models of wayfinding in emergency evacuations. *European journal of operational research* 105, 371–389.
- Lovreglio, R., Ronchi, E., Borri, D., 2014. The validation of evacuation simulation models through the analysis of behavioural uncertainty. *Reliability Engineering & System Safety* 131, 166–174.
- Lu, L., Chan, C.Y., Wang, J., Wang, W., 2017. A study of pedestrian group behaviors in crowd evacuation based on an extended floor field cellular automaton model. *Transportation Research Part C: Emerging Technologies* 81, 317–329.
- Meister, J., 2007. Simulation of crowd dynamics with special focus on building evacuations. Master’s thesis. University of Applied Sciences Wedel. Wedel, Germany.
- Olsson, P.Å., Regan, M.A., 2001. A comparison between actual and predicted evacuation times. *Safety science* 38, 139–145.
- Pan, X., Han, C.S., Dauber, K., Law, K.H., 2007. A multi-agent based framework for the simulation of human and social behaviors during emergency evacuations. *Ai & Society* 22, 113–132.
- Pelechano, N., Malkawi, A., 2008. Evacuation simulation models: Challenges in modeling high rise building evacuation with cellular automata approaches. *Automation in construction* 17, 377–385.
- Proulx, G., 2002. Movement of people: the evacuation timing, in: SFPE handbook of fire protection engineering, third ed.. National Fire Protection Association, Quincy, MA. chapter 3-13, pp. 3–342–366.
- Railsback, S.F., Lytinen, S.L., Jackson, S.K., 2006. Agent-based simulation platforms: Review and development recommendations. *Simulation* 82, 609–623.
- Richter, K.F., Shi, M., Gan, H.S., Winter, S., 2013. Decentralized evacuation management. *Transportation Research Part C: Emerging Technologies* 31, 1–17.
- Rinne, T., Tillander, K., Grönberg, P., 2010. Data collection and analysis of evacuation situations. Research Notes 2562. VTT Technical Research Centre of Finland. Espoo, Finland.
- Sano, T., Yoshida, Y., Takeichi, N., Kimura, T., Minegishi, Y., 2011. Experimental study of crowd flow passing through simple-shaped room and validation for an evacuation simulator, in: Peacock, R.D., Kuligowski, E.D., Averill, J.D. (Eds.), *Pedestrian and Evacuation Dynamics*. Springer, pp. 587–599.
- Schadschneider, A., Eilhardt, C., Nowak, S., Will, R., 2011. Towards a calibration of the floor field cellular automaton, in: Peacock, R.D., Kuligowski, E.D., Averill, J.D. (Eds.), *Pedestrian and Evacuation Dynamics*. Springer, pp. 557–566.
- Shiwakoti, N., Sarvi, M., 2013. Enhancing the panic escape of crowd through architectural design. *Transportation Research Part C: Emerging Technologies* 37, 260–267.
- Van Den Berg, J., Guy, S.J., Lin, M., Manocha, D., 2011. Reciprocal n-body collision avoidance, in: *Robotics Research*. Springer, pp. 3–19.
- Walker, J.M., 2013. Informe Técnico de Evaluación, Simulacro Macrozona de Terremoto y Tsunami, Evacuación del Borde Costero, Regiones de Arica y Parinacota, Tarapacá, Antofagasta y Atacama. Technical Report. Oficina Nacional de Emergencia del Ministerio del Interior y Seguridad Pública - ONEMI. Santiago, Chile. [In spanish].
- Wang, H., Mostafizi, A., Cramer, L.A., Cox, D., Park, H., 2016. An agent-based model of a multimodal near-field tsunami evacuation: decision-making and life safety. *Transportation Research Part C: Emerging Technologies* 64, 86–100.

- Wilensky, U., 1999. NetLogo. <http://ccl.northwestern.edu/netlogo/>. Center for Connected Learning and Computer-Based Modeling, Northwestern University. Evanston, IL. URL: <http://ccl.northwestern.edu/netlogo/>.
- Yang, L.Z., Zhao, D.L., Li, J., Fang, T.Y., 2005. Simulation of the kin behavior in building occupant evacuation based on cellular automaton. *Building and Environment* 40, 411–415.
- Yin, W., Murray-Tuite, P., Ukkusuri, S.V., Gladwin, H., 2014. An agent-based modeling system for travel demand simulation for hurricane evacuation. *Transportation Research Part C: Emerging Technologies* 42, 44–59.
- Zhang, J., Song, W., Xu, X., 2008. Experiment and multi-grid modeling of evacuation from a classroom. *Physica A: Statistical Mechanics and its Applications* 387, 5901–5909.